

**DISTRIBUTED ENERGY RESOURCES IMPACT ON CVR**

---

**3.1 Introduction**

The conventional distribution systems are facing numerous operation and control issues since the last few decades due to widespread DER deployment and shift in energy paradigm. To address the control aspects, this chapter has discussed the impact of VVC operation with CVR in the presence of DER which is the third technical barrier, as described in *chapter 1*. In this context, researchers [51], [87] have analyzed the combined impact of CVR and various levels of DG penetration and mitigation of low voltage violation during deeper voltage reduction. In [78], the effect of photovoltaic DER penetrations during CVR is investigated with various cases of VVC, but the ability of PV inverter is not fully utilized. Besides, it lacks the cooperation of the distributed renewable sources due to intermittent behavior and slow operation of traditional Volt/VAR controlling devices. Hence, the impact of PV inverters as VAR support and voltage regulation device has been analyzed in [19], [21], [82], [91],[95]. However, these studies have not analyzed the voltage control through PV inverter during CVR. The combined effect of CVR and PV inverters has been performed in [20], [58], [68], [77]. In [68], a slow and fast time scale based VVC scheme for CVR is proposed with the objective of minimizing total energy consumption. The optimal reactive power support through PV inverter with the objective of minimizing voltage deviation has been presented in [88]. The closed-loop CVR problem has been analyzed through reactive power support from PV inverter in [20]. However, this method has been tested only for a limited voltage reduction range on the simple balanced network considering the impedance load model.

An attempt has been made in this investigation to address the second and third technical barriers for which a smart grid-enabled CVR scheme for VVC has been proposed. In order to control the tap position of OLTC/ AVR, a well-established LDC scheme has been employed. The limits of tap change and CB switching for daily operation have been considered in control algorithms. Besides, CVR in association with PV system has been implemented to achieve a greater saving in peak demand and energy consumption even during deeper voltage reduction. In addition, reactive power compensation has been done through PV inverters to control the lower voltage violation. The desired reactive power has calculated and controlled through Volt/VAR droop control mechanism. The effect of inverter losses due to reactive current generation during reactive power support has also been included. The moving cloud transient effect has been considered while developing the solar PV model. The proposed scheme has been tested on unbalanced radial distribution network with voltage-dependent composite ZIP load models for peak demand hours and whole day operation. The effect of various types of loading such as residential, commercial and industrial are also incorporated in the load model.

### **3.2 Overview of DER**

Distributed energy resources are known as various names as distributed generation, onsite power generation source, etc. DGs are broadly divided into two categories as renewable and non-renewable DERs. Further classification can be inverter type DER which generally operates at unity power factor, and other is synchronous or non-synchronous machine having 0.9 leading power factors [51]. Rapid development in the field of power electronics and control, it is quite possible that renewable DERs can provide not only active power but reactive power support also. Due to global popularity and the potential of fast controlling reactive power with fine-tuned var output, the grid-connected solar PVs

with smart inverter considered as a DER in this chapter. For performing power flow calculations, PV source has been considered as a PQ node with the known value of real and reactive powers with their limits in equations below:

$$P_{DER,Min} \leq P_{DER} \leq P_{DER,Max} \quad (3.1)$$

$$Q_{DER,Min} \leq Q_{DER} \leq Q_{DER,Max} \quad (3.2)$$

$$(P_{DER})^2 + (Q_{DER})^2 \leq (S_{DER}^{rated})^2 \quad (3.3)$$

With the equations of (3.1), (3.2) and (3.3) power facility curve can be defined.

$$|Q_{DER}^{Inj}| \leq Q_{DER,Max} = \sqrt{(S_{DER}^{rated})^2 - (P_{DER})^2} \quad (3.4)$$

It is quite possible to develop a variable solar DER VAR source ( $\Delta Q_{DER}^{Inj}$ ) model for voltage regulation. The injected reactive power ( $Q_{DER}^{Inj}$ ) must satisfy the equation (3.4) and other constraints.

### 3.3 Voltage regulation through PV Smart Inverter

PV inverter used for the integration of PV panel commonly known as conventional PV inverter. However, PV inverters having advanced functionality such as the ability to participate in VAR support, islanding deduction and power management are referred as smart inverter. The ability to provide reactive power support and/or performed as VAR compensators enlarge the PV inverters contribution significantly in the improvement of distribution operation, maintain the voltage profile within the acceptable range and minimize the system losses. The detailed description of smart inverter operation has already explained in *chapter 1 subsection 1.4.2.3*. In general, PV smart inverter operates in two quadrants with five modes as shown in Figure 3.1 and explains below [88].

Mode 1- Only active or real power (P), Q=0

Mode 2- Active power, With Inductive Q power

Mode 3- No active power (P=0), Only Inductive Q

Mode 4- Active power (P), Capacitive Q

Mode 5- No active power (P=0), Only Capacitive Q

Modes 1, 2, and 4 will operate at day time where solar irradiation is available while mode 3, 5 enabled in the night, or absence of sunlight.

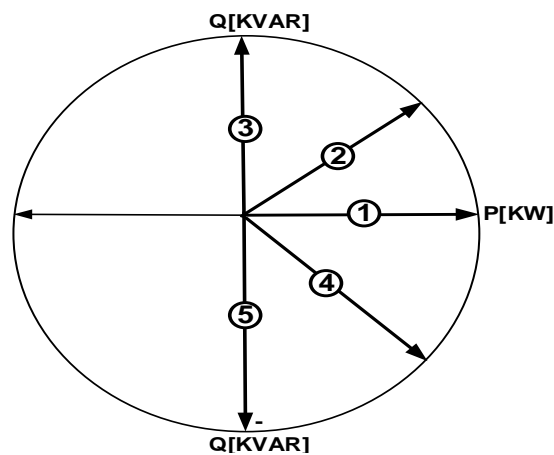


Figure 3.1 PV Inverter P/Q Capability Curve

### 3.4 Mathematical Formulation and Control Methodology

The basic objective of this investigation is to save energy in ADN. This objective can be fulfilled by reducing the demand of the system by lowering the voltage of the network. Energy savings by reducing the voltage is an advance attribute of the integrated VVC mechanism. Therefore, in this section mathematical formulation and control approach to enable the CVR operation through VVC is delineated as under.

#### 3.4.1 Mathematical Formulation

The power demand at the source substation is the sum of total real power loads and the real power losses on lines/cables ( $P_{loss}^{lines/cables}$ ), transformers ( $P_{loss}^{transformers}$ ) and inverters ( $P_{loss}^{inverter}$ ) as expressed by equations (3.5 - 3.7).

$$P_{Demand} = \sum (P_{Load} + P_{Loss}) \quad (3.5)$$

where

$$P_{load} = \sum_{\phi \in a,b,c} \sum_{k=1}^{nl} (P_{L,k}(V_k))_{\phi} \quad (3.6)$$

and

$$P_{loss} = \sum (P_{loss}^{lines/cables} + P_{loss}^{transformers} + P_{loss}^{inverter}) \quad (3.7)$$

From equation (3.6), it can be observed that the real power demand at a node is dependent on its voltage. Transformer core losses depend upon the voltage, whereas transformer winding and line losses mainly depend upon current flow. Inverter losses take place due to electronic circuitry and flow of reactive current when PV inverter absorbs/inject the reactive power. Therefore, total active power losses may decrease or increase with reduced voltage. Moreover, it also depends on several other factors such as network topology, load models, and load types.

- The reduction of voltage is obtained through maneuvering the tap position of OLTC transformer and automatic voltage regulators. Equations (3.8) and (3.9) express the regulated output voltage from OLTC/AVR.

$$V_{tr} = a_{tr} V_P \quad (3.8)$$

$$V_{tr} = \left\{ 1 \pm \left( \frac{\Delta V_{tr}}{100} \right) \times \text{Tap} \right\} V_P \quad (3.9)$$

- Daily tap operation of OLTC/AVR is governed by equation (3.10) to prevent the degradation of the life cycle of voltage regulation devices.

$$\sum_{h=1}^{24} N_{tr,h}^i \leq N_{tr,max}^i \quad (3.10)$$

- Reactive power supplied by CBs at each switching operation is defined by the equation (1.12) and daily switching operation of CBs should follow the relation (3.11).

$$\sum_{h=1}^{24} N_{sw,h}^i \leq N_{sw,max}^i \quad (3.11)$$

Reactive power compensation from PV inverter is determined by advanced Volt/VAR droop characteristics as shown in Figure 3.2. This characteristic can further be expressed as relation (3.12) where,  $Q_T^{inv,max}$  is governed by equation (1.16).

$$Q_T^{inv}(V) = \begin{cases} Q_T^{inv,max} & V < V_1^{P_1} \\ \frac{V - V_1^{P_1}}{V_1^{P_1} - V_2^{P_2}} Q_T^{inv,max} & V_1^{P_1} \leq V < V_2^{P_2} \\ 0 & V_2^{P_2} \leq V \leq V_3^{P_3} \\ -\frac{V - V_3^{P_3}}{V_4^{P_4} - V_3^{P_3}} Q_T^{inv,max} & V_3^{P_3} < V \leq V_4^{P_4} \\ -Q_T^{inv,max} & V > V_4^{P_4} \end{cases} \quad (3.12)$$

- According to ANSI, the node voltage magnitude limit is defined by the following equation.

$$V_{i,T}^{\min} \leq V_{i,T} \leq V_{i,T}^{\max} \text{ or } 0.95\text{pu} \leq V_{i,T} \leq 1.05\text{pu} \quad (3.13)$$

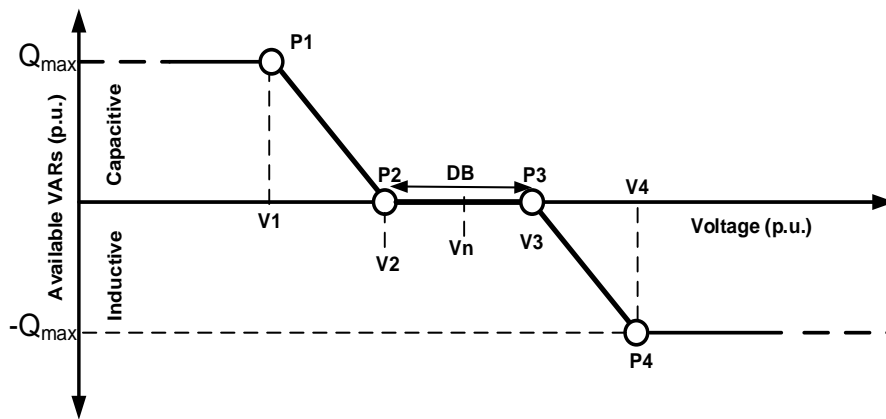


Figure 3.2 Volt/VAR droop characteristics

### 3.4.2 Control Methodology

Voltage and reactive power flow in the network are governed by controlling of OLTC/regulator, CBs, and smart inverter. The functional control of OLTC/regulator and CB has been already described in *chapter 2*, section 2.3.1 and section 2.3.2. The PV inverter control strategy has been discussed as under.

#### 3.4.2.1 Smart PV inverter control

In this work, inverter control circuitry deals mainly with calculation of the desired reactive power at each time period,  $T$ . In order to determine it, a droop characteristics based scheme has been utilized. The Volt/VAR droop characteristics are shown in Figure 3.2. It is piecewise linear to the voltage and also changes dynamically due to its dependency on the  $Q_T^{inv,max}$ . The droop characteristics are obtained by defining the four points ( $P_1, P_2, P_3$  &  $P_4$ ) parameters and dead band (DB). The DB is defined as the width between points  $P_2$  and  $P_3$  in terms of voltage range symmetrical to  $V_n$ . In the DB range, inverter neither absorbs nor injected the VAR. Below the point  $P_2$  ( $V_2^{P_2}$ ), the inverter starts injecting reactive power to the grid. However, when a voltage is above point  $P_3$  ( $V_3^{P_3}$ ), the inverter absorbs reactive power from the grid. The amount of reactive power injected/absorbed by the inverter is determined using equation (3.12).

## 3.5 Implementation of VVC Scheme

The control approach for various controllers is well explained earlier in *section 3.4*. In order to estimate the energy savings and CVR factor, VVC is carried out in three different modes with developed controllers as delineated under:

### 3.5.1 Mode 1 (Without CVR or Normal Operation)

In this mode, VVC operation is performed within the upper range of the service voltage known as normal, i.e. No- CVR operation. End of line (EOL) / regulated voltages in

regulator control are set between 121-126V with  $V_{base}$  of 120V. Shunt capacitors of CB are fixed in nature. Only LTC/regulator controllers are active in this mode.

### 3.5.2 Mode 2 (Only CVR)

In this mode, VVC operation is carried out with only CVR scheme without any additional power support. CVR scheme is enabled through LDC with the setting of regulated voltages in the lower half range (114V-119V) of the service voltage. CBs are switchable in this mode. Only inverter controller is inactive in this mode. The level of voltage reduction is increased to achieve higher energy savings with only CVR mode. However, this may lead to violation of the minimum voltage limits at some points of the distribution feeder.

### 3.5.3 Mode 3 (CVR with PV)

In order to achieve higher energy saving through deeper CVR and maintain the minimum allowable voltage throughout the feeder length, an additional power source is required. Therefore, in this mode, CVR is enabled with additional power support from PV system. The required additional active/reactive power is provided through PV system with the advanced functioning of solar PV inverter. The cloud transient effect is considered in PV power output.

The implementation of three modes has been done in three stages as shown in Figure 3.3 and explained as under.

- (i) The first stage deals with the development of the network model of considered test system including controllers. After that, the VVC operation mode is selected from the control panel and the required parameters such as EOL/ $V_{reg}$  are set. The controllers for selected mode are enabled.
- (ii) The second stage is mainly based on the execution of control actions, power flow analysis and verification of solution limits. Control actions execution for enabled

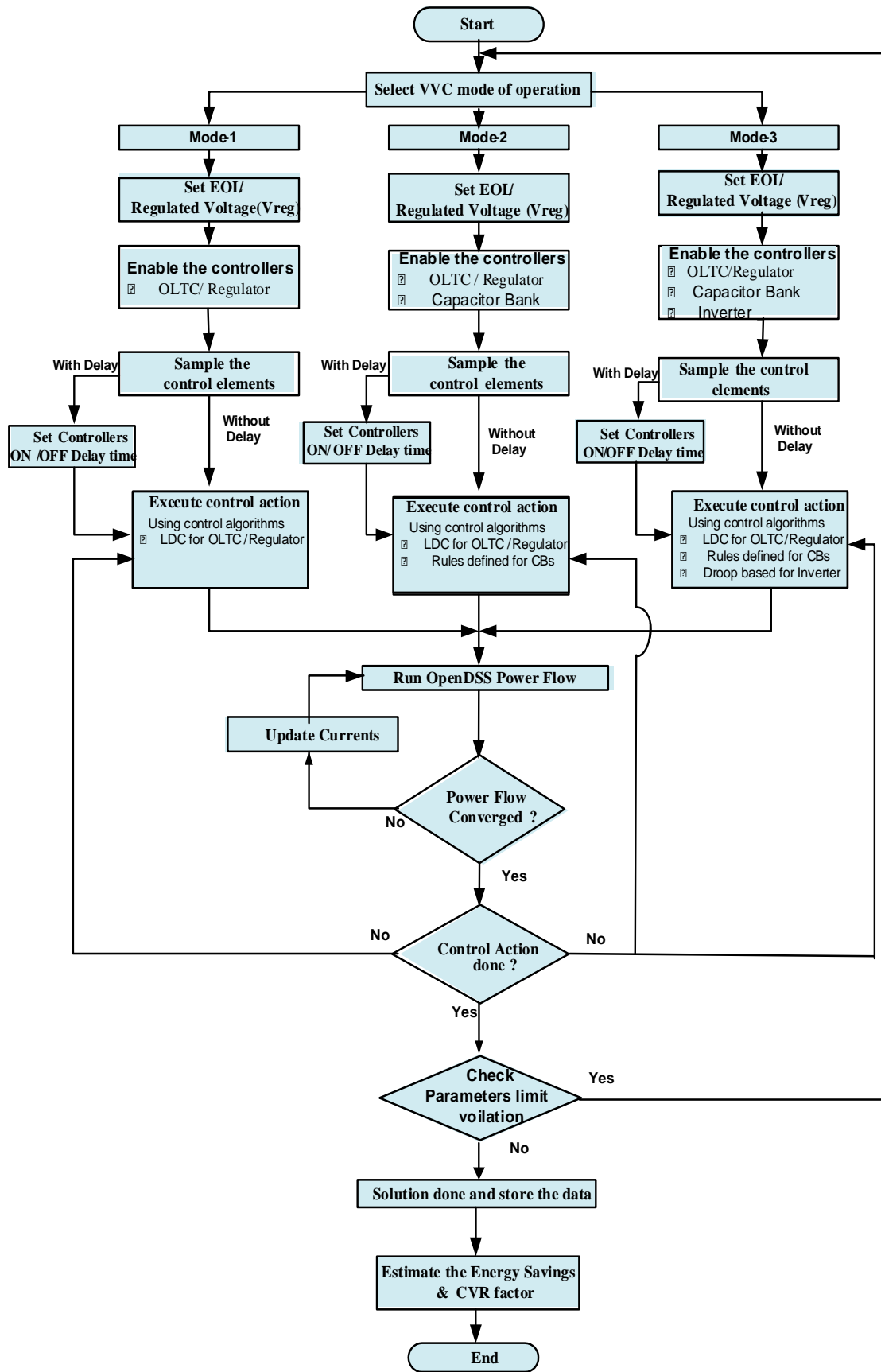


Figure 3.3 Flow chart of VVC mode of operation

controllers can be set either simultaneously or with some delayed action. The stepwise procedure of this stage is delineated under:

- Sample the control elements inputs.
- Set the controllers ON/OFF time delay, if the delay in control queuing is enabled.
- Determine governing VVC parameters using control algorithms.
- Calculate the required tap settings for OLTC/AVR through LDC using equation (2.11).
- Perform ladder iterative method for load flow analysis and obtain the feasible solution.
- Find CB switching step and reactive power support from inverter using equation (1.16) and (3.12) respectively.
- If control action is completed, then verify the violation limits else again execute control action.
- If obtained results are within limits, then accept the solution and store the data, if not, go to the selection of VVC mode of operation.

(iii) In the third stage, estimation of energy savings and CVR factor is performed through data obtained using the equations (2.1) and (2.2) respectively.

### **3.6 Simulations and Result Discussion**

In this section, the simulation results of test cases have been presented and discussed. The proposed smart grid-enabled CVR methodology has been validated in the presence of PV based DER using simulation method.

#### *3.6.1 Test System and Modelling*

For the assessment of CVR effect, a modified IEEE 123 node distribution test feeder [114] has been considered as shown in Figure 3.4. Ratings and parameters of VVC devices have been shown in Table 3.1.

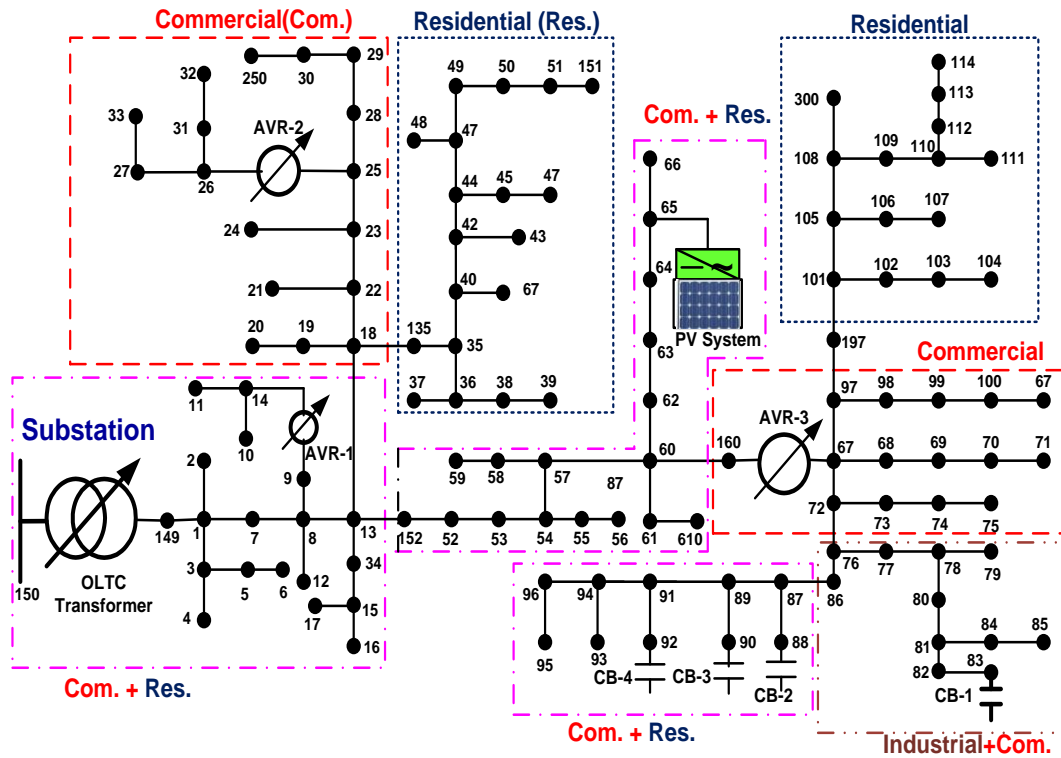


Figure 3.4 Modified IEEE 123 node distribution test feeder

Modeling of the distribution network, controllers, PV system and power flow calculations have been done and simulated on OpenDSS platform[28]. However, the control algorithms have been written in MATLAB and interfaced with OpenDSS model.

Before performing simulations of the test systems, the following assumptions have been incorporated:

- The communication system is working well, and its delay effect has been ignored during the execution of CVR.
- Data up-gradation duration of 15 minutes has been taken for AMI system and field devices.
- ZIP load models are considered throughout the distribution network with and without CVR operation. ZIP coefficients are depicted in Table 3.2. The detailed representation of ZIP load model has been explained in *chapter 1* using equations (1.17) – (1.20) respectively.

- The load allocation factor for distributed load is set to 1 in OpenDSS inbuilt allocation algorithm.
- Load demand profile with active and reactive power demand multipliers for 24 hours with 15 minutes interval of a typical day has been considered, and it is shown in Figure 3.5.
- The switching effect is neglected during the operation of switched shunt capacitor banks. However, switching time has been incorporated, taking a suitable time delay in control queuing.

**Table-3.1.** Ratings and Parameters of VVC devices

Device	Phase (Ph) /Connection	Location At/Between node/rating		Tap range / CB step per phase /Inverter $S_{max}$	Maximum daily tap change/ CB switching operation per phase	
<b>OLTC</b>	3-Phase (a-b-c),Wye	150 - 149		+16 to -16	5	
<b>AVR-1</b>	1-Phase, a	9-14		+16 to -16	5	
<b>AVR-2</b>	2-Phase, a, c	25-26		+16 to -16	5	
<b>AVR-3</b>	3-Phase a,b,c	160-67		+16 to -16	5	
<b>CB-1(kVAR)</b>	3- Phase, a,b,c	83	200/Phase	0-4	3	
<b>CB-2(kVAR)</b>	1- Phase, a	88	50/ Phase	0-1	3	
<b>CB-3(kVAR)</b>	1- Phase, b	90	50/ Phase	0-1	3	
<b>CB-4(kVAR)</b>	1- Phase, c	92	50/ Phase	0-1	3	
<b>PV Inverter</b>	<b>KVA</b>	3- Phase, a-b-c	65	200	200	---
	<b>Efficiency (<math>\eta_{inv}</math>)</b>	0.985, (when it is injecting either P or Q only)				
		0.97, (when it is injecting both P and Q simultaneously).				
<b>Volt/VAR droop characteristics points</b>	Point P1 voltage ( $V_1^{P_1}$ ) = 0.945 p.u., Point P2 voltage ( $V_2^{P_2}$ ) = 0.95 p.u., Point P3 voltage ( $V_3^{P_3}$ ) = 1.05 p.u., Point P4 voltage ( $V_4^{P_4}$ ) = 1.06 p.u., Dead Band (DB) range = Between point P2 and P3, 0.1 p.u.					

**Table-3.2. ZIP Load Model Parameters**

Loading Type	ZIP Coefficients		Node Number
	[53]		
<b>Residential</b>	$Z_p = 0.85$ $I_p = -1.12$ $P_p = 1.27$	$Z_q = 10.96$ $I_q = -18.73$ $P_q = 8.77$	2,4,5,6,7,10,12,16,35,37,38,39,41, 42,43,45,46,47,48,49,50,51,52,53, 55,56,58,59,60,65,94,95,96,102,1 03,104,106,107,109,111,112,113, 114
<b>Large Commercial</b>	$Z_p = 0.47$ $I_p = -0.53$ $P_p = 1.06$	$Z_q = 5.30$ $I_q = -8.73$ $P_q = 4.43$	62,63,64, 66,80,82,85
<b>Small Commercial</b>	$Z_p = 0.43,$ $I_p = -0.06,$ $P_p = 0.63$	$Z_q = 4.06,$ $I_q = -6.65,$ $P_q = 3.59$	1,9,11,17,19,20,22,24,28, 29,30,31,32,33,34,68,69,70,71,73 ,74,75,83,84,87,88, 90,92,98,99,100
<b>Industrial</b>	$Z_p, I_p = 0,$ $P_p = 1$	$Z_q, I_q = 0,$ $P_q = 1$	76,77,79,86

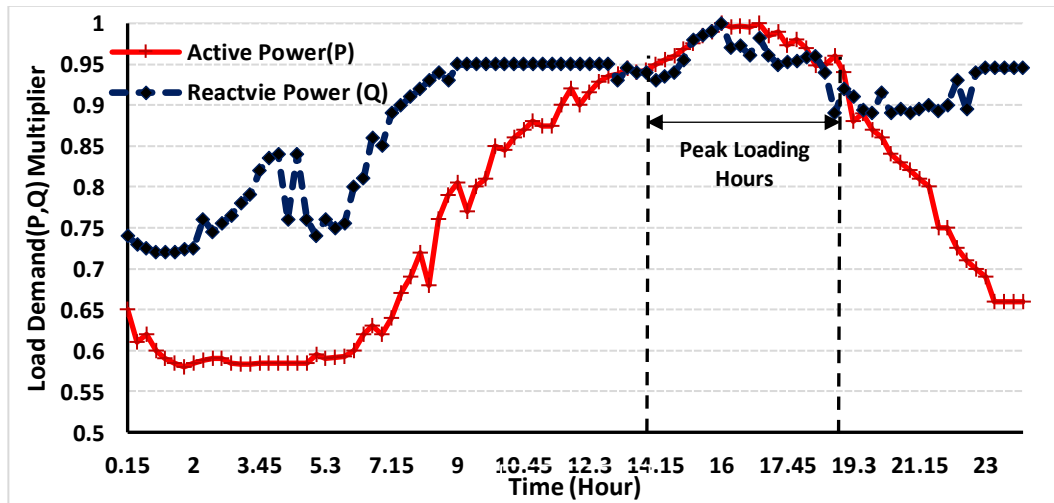


Figure 3.5 Load demand profile for 24 hours

### 3.6.2 Case Study

The Modified IEEE 123 node test system is simulated for two cases in the above mentioned three modes of VVC operation:

- Case. I- Peak Demand Reduction
- Case. II- Daily Energy Demand Reduction

### 3.6.2.1 Case. I- Peak Demand Reduction

Peak demand reduction through CVR is investigated in this case study. The demand above 95% of the highest active power demand has been considered as the peak demand hours in the present study. The duration of such load on the test system under consideration spreads from 14:15 to 19:00 hours which approximates to 5 hours. The load profile of a typical day is shown in Figure 3.5 along with peak demand hours. The effect of CVR on peak demand reduction in three modes of VVC operation has been analyzed under this loading condition.

- *Mode 1:* The simulation results for the peak demand duration without CVR (normal operation) have been obtained with the application of VVC to maintain 124V regulated voltage with the help of LDC settings. The results of this mode of operation are shown in the second column of Table 3.3. The active power demand of the system is shown in Figure 3.6 for the considered duration.

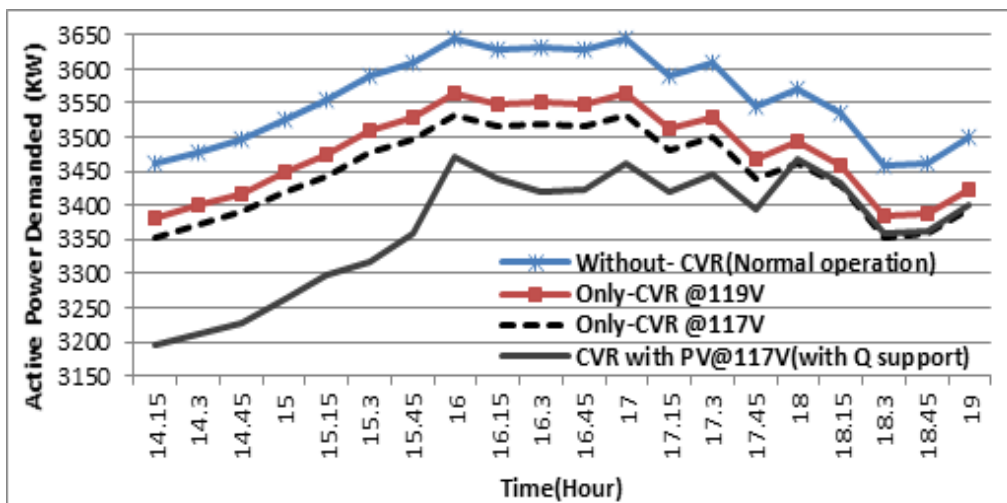


Figure 3.6 Active power demand at feeder head in all modes of operation in Case-I (Peak demand Hours)

- Mode 2*: The test system, for this mode of operation, has been simulated for two different regulated voltages of 119V and 117V. The results have been given in the third column of Table 3.3. From results, it can be observed that a significant reduction in energy demand about 1.96 % and 2.81% is achieved at 119V and 117V, respectively in comparison to Mode 1. However, the energy losses have been slightly (about 3.2 % for 119V and 4.7 % for 117 V) increased. The increased losses are not so significant and can be overlooked because reductions in energy consumption are sufficiently higher than the increased energy losses. From Figure 3.7, it is further observed that there are no violations of minimum voltage limit (below 0.95 p.u.) at 119V. However, during deeper voltage reduction (CVR at 117V regulated voltage) the minimum voltage limits have been violated. The maximum voltage deviation from permissible voltage (0.95p.u.) is 0.006 p.u. The lowest voltage of 0.944 p.u. has been observed at node 65. Figure 3.6 shows the total active power demanded from the substation. The  $CVR_{FE}$  is 0.486 and 0.497 for two regulated voltages respectively.

**Table-3.3** Simulation results of Case I (Peak Demand Reduction)

Energy (E) Terms	Mode-1	Mode-2		Mode-3	
	Without CVR (124V)	Only-CVR		CVR with PV (117V)	
		(119V)	(117V)	Without Q support	With Q support
<b>Econsumption (MWh)</b>	17.747	17.400	17.248	16.845	16.842
<b>Energy losses, MWh, (%)</b>	0.446 (2.51)	0.460 (2.59)	0.467 (2.63)	0.449 (2.530)	0.4440 (2.501)
<b>Esaving, kWh, (%)</b>	--	347 (+1.96)	499 (+2.81)	901.7 (+5.08)	904.417 (+5.09)
<b><math>\Delta</math>Losses, kWh, (%)</b>	--	+14 (+03.2)	+21 (+4.7)	-3.244 (+0.72)	+1.840 (-0.41)
<b>Lowest Voltage ( p.u.), (Node)</b>	1.00 (65)	0.9634 (65)	0.9441 (65)	0.9464 (65)	0.9500 (63)
<b><math>CVR_{FE}</math></b>	--	0.486	0.497	0.900	0.903

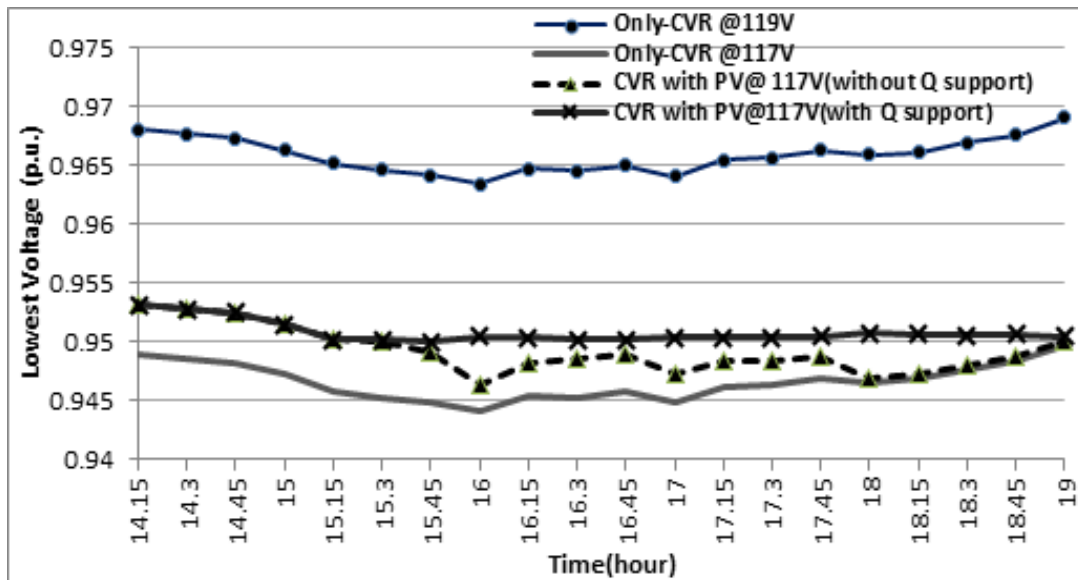


Figure 3.7 Minimum node voltage profile in all modes of operation in Case-I (Peak demand Hours)

- Mode 3:* In this mode, the test system has been further simulated for two subcases as PV power injection with and without reactive power support from PV inverter. The allocation of PV system in the network has been chosen based on the lowest node voltage profile. The lowest voltage has been observed at node 65 as shown in Table 3.3. Therefore, a residential PV system with 200 KVA rating of the smart inverter has been placed at node 65. The simulated results are depicted in fourth column of Table 3.3. It can be observed from the table that about 5.08% reduction in energy demand is achieved during CVR (with PV without Q support). However, the minimum voltage limit violated during the time span 15:15 to 19:00 as shown in Figure 3.7. VVC operation with CVR and PV with Q support mode reported 5.09 % reduced energy demand and 0.41% reduction in energy losses maintaining voltage profile within ANSI range. Figure 3.7 clearly demonstrates the improvement in voltage under this mode of operation. The additional reactive power support is controlled by Volt/VAR droop characteristics as shown in Figure 3.2. The droop characteristics assist in determining the appropriate amount of reactive power to be injected from the inverter to maintain the voltage within the desired

range. In the present case, droop control operation has been carried out in the range prior to point P<sub>3</sub> of droop characteristics. Since the range between point P<sub>2</sub> and P<sub>3</sub> is dead band range, the inverter starts injecting the reactive power prior to point P<sub>2</sub> (i.e., voltage below 0.95 p.u.) until desired reactive power is injected. Figure 3.8 shows the active and reactive power fed by PV system along with its droop control. Active power losses and inverter losses are shown, in Figure 3.9, for this mode. From Figure 3.9, it is observed that inverter losses increased when it injected the reactive power (excluding time span 14:15 to 15:00 because, during this time span, Q support is zero). However, increased inverter losses due to Q support does not affect the net system active power losses. The  $CVR_{fE}$  for subcases without and with reactive power support has been found to be 0.900 and 0.903 respectively as shown in Table 3.3. It can be comprehended from the aforesaid results that the maximum peak demand reduction would be achieved by the application of CVR with PV system, extending the reactive power support. The CVR factor estimated in this work measures the effectiveness of deployment of CVR. This factor also indicates that operation in Mode-3 performed better than Mode-2.

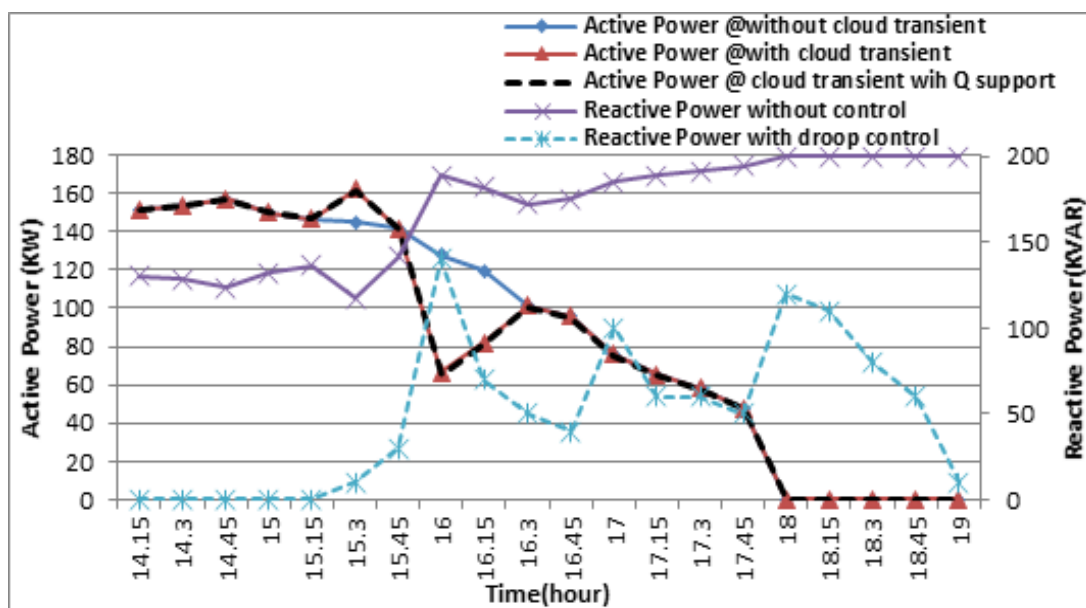


Figure 3.8 Real and reactive power feed by PV system during Mode-3 operation in Case-I (Peak demand Hours)

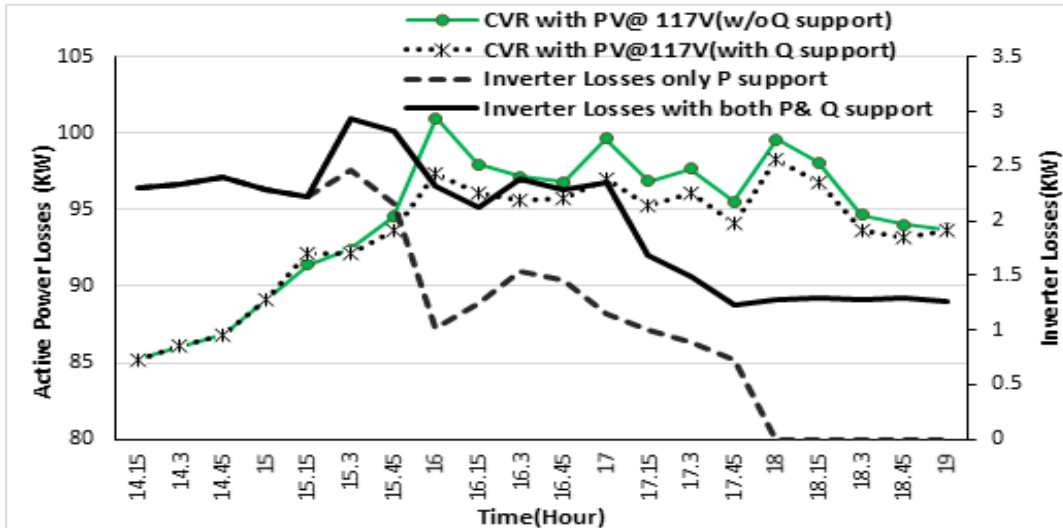


Figure 3.9 Active power losses and inverter losses during Mode-3 operation in Case-I (Peak demand Hours)

### 3.6.2.2 Case. II- Daily Energy Demand Reduction or Daily Energy Savings

In this case study, CVR scheme is tested with the aim of a reduction in daily energy demand. The proposed scheme is deployed on the same system for a maximum demand day of a week. The entire day's load profile of the day shown in Figure 3.5 has again been used to demonstrate the effect of all the three modes of VVC operation. The simulated results related to energy consumption and losses are shown in Table 3.4. Total active power demand and lowest node voltage profile during whole day operation are shown in Figure 3.10 and Figure 3.11 respectively. The obtained simulation results from each mode are discussed as under:

- *Mode 1:* The simulation results during without CVR operation is obtained with the execution of VVC at 124V regulated voltage. Table 3.4 shows the total active energy demand and active power losses. Figure 3.10 shows the active power demand of the system for the considered duration.
- *Mode 2:* The test system has been simulated for two regulated voltages of 119V and 117V as shown in Table 3.4. From results, it can be demonstrated that during CVR, significant energy savings amounting to 1.9% and 2.83% are achieved. However, the

energy losses have been increased to 2.85 % and 4.08 %, respectively. The increased losses are included in achieved total energy savings. From Figure 3.11, it is observed that the minimum voltage limit is violated at some nodes of the feeder end during CVR operation at 117V. The value of  $CVR_{fE}$  is 0.47 and 0.50 respectively for two regulated voltages.

- *Mode 3:* In this mode, the test system is simulated with CVR and PV at 117V regulated voltage with and without reactive power support. The energy savings in this mode is increased to 4.727 % and losses are almost equal to the Mode 1. The feeder voltage profile is maintained within limits with the injection of PV power during CVR operation at 117V as shown in Figure 3.10. The power loss variation throughout the day has been shown in Figure 3.12. The PV power profile during the entire day is shown in Figure 3.13. The calculated  $CVR_{fE}$  is 0.89 which is higher than Mode 2.

**Table-3.4-** Simulation results of Case II (Whole day operation)

Energy (E) Terms*	Mode-1	Mode-2		Mode-3	
	Without- CVR (124V)	Only-CVR		CVR with PV (117V)	
		(119V)	(117V)	Without Q support	With Q support
<b>Econsumption (MWh)</b>	68.159	66.863	66.232	64.9397	64.9370
<b>Energy losses, MWh, (%)</b>	1.469 (2.15)	1.511 (2.21)	1.5292 (2.24)	1.4783 (2.168)	1.4732 (2.161)
<b>Esaving, MWh, (%)</b>	--	1.30 (+1.90)	1.93 (+2.83)	3.2192 (+4.724)	3.2219 (+4.727)
<b><math>\Delta</math>Losses, kWh, (%)</b>	--	+42 (+2.85)	+60.2 (+4.08)	+9.098 (+0.61)	+4.08 (+0.272)
<b>Lowest Voltage ( p.u.), (Node)</b>	1.00 (65)	0.9634 (65)	0.9441 (65)	0.9464 (65)	0.9500 (63)
<b><math>CVR_{fE}</math></b>	--	0.47	0.50	0.8366	0.8374

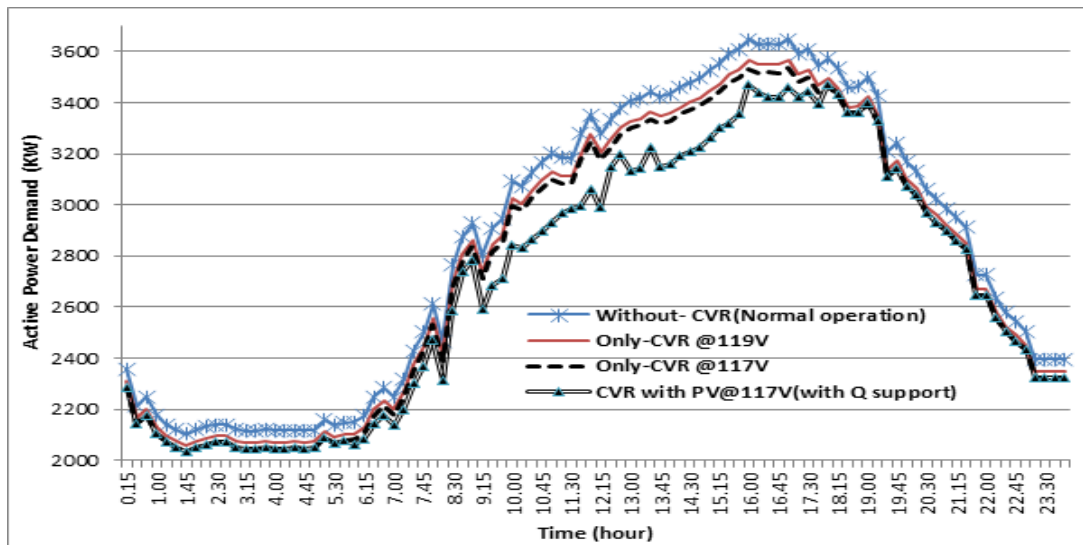


Figure 3.10 Active power demand at feeder head in all modes of operation in Case-II (whole day operation)

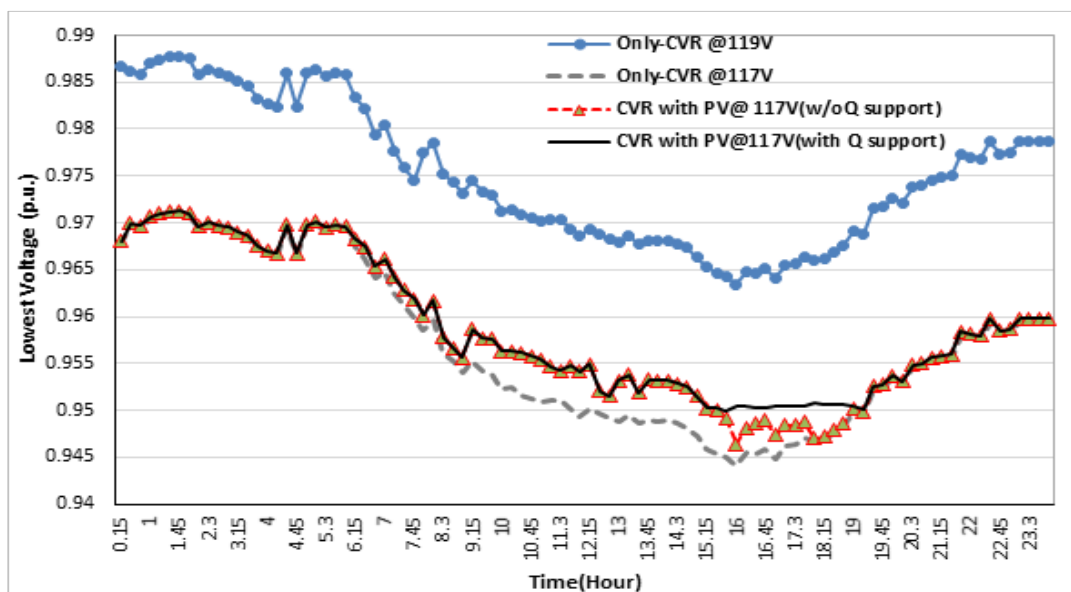


Figure 3.11 Minimum node voltage profile in all modes of operation in Case-II (whole day operation)

Entire day tap positions of OLTC and AVR are shown in Figure 3.14 – Figure 3.17 respectively. It is observed that tap positions have been reduced with the enabling of CVR. Per phase tap operations for the day for every device are limited to the maximum five times, which are clearly portrayed in Figure 3.14 to Figure 3.17 also. The CB switching operations for the day are also restricted up to three times per phase and it has been shown in Table 3.5.

From the above-discussed case studies, it is demonstrated that considerable energy consumptions and peak power demand can be reduced with CVR operation. To achieve higher energy savings through deeper CVR operation is not a secure way. Therefore, deployment of CVR scheme with PV system is advisable.

**Table-3.5** CBs switching operation status

Device \ Mode	Mode-1	Mode-2				Mode-3		
	With out CVR	Only- CVR (119V)		Only- CVR (119V)		CVR with PV (117V)		
<b>Time Duration</b>	00:24	00.15: 6.00	6.15: 24.00	00.15: 6.00	6.15: 24.00	00.15: 6.00	6.15: 24.00	
<b>CB-1</b>	<b>Phase-a</b>	4	2	3	2	3	2	3
	<b>Phase-b</b>	4	2	2	2	2	2	2
	<b>Phase-c</b>	4	2	3	2	3	2	3
<b>CB-2</b>	1	0	1	0	1	0	1	
<b>CB-3</b>	1	0	1	0	1	0	1	
<b>CB-4</b>	1	0	1	0	1	0	1	

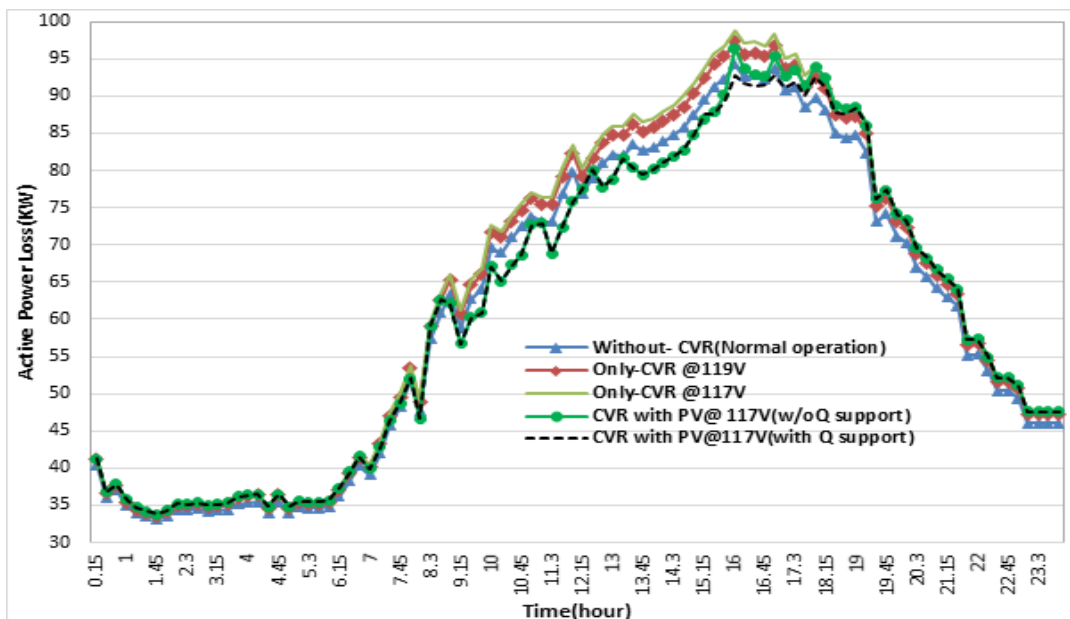


Figure 3.12 Active power losses during Mode-3 operation in Case-II (whole day operation)

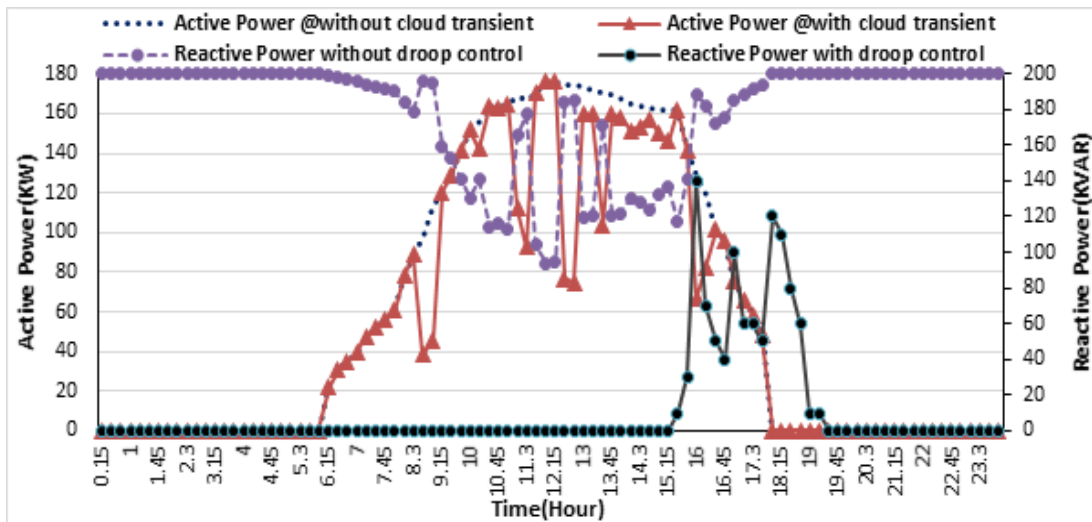


Figure 3.13 Active and reactive power feed by PV system during Mode-3 operation Case-II (whole day operation)

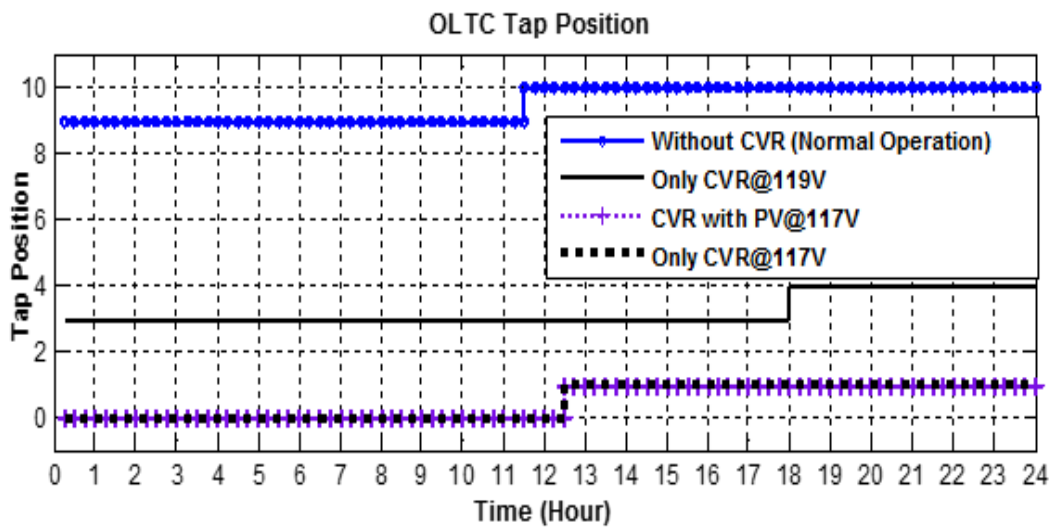


Figure 3.14 Tap Position of OLTC transformer in Case II for whole day operation

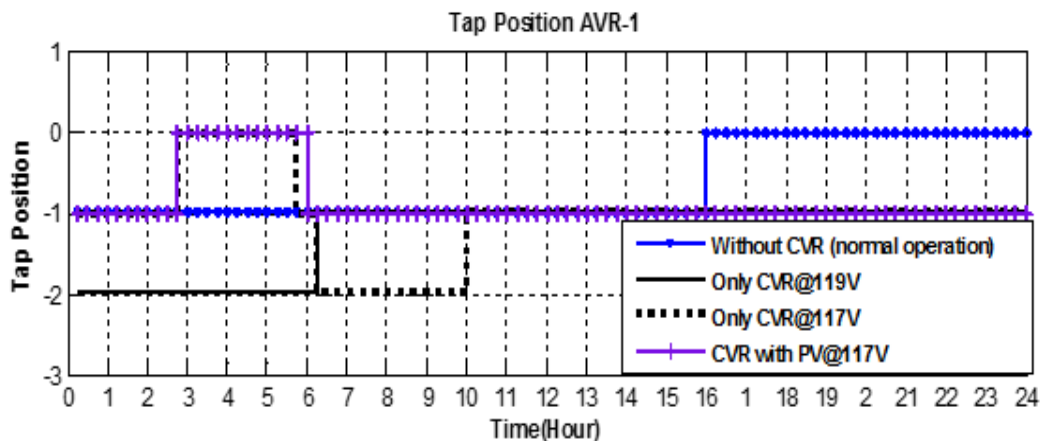


Figure 3.15 Tap Positions of AVR-1 in Case II for whole day operation

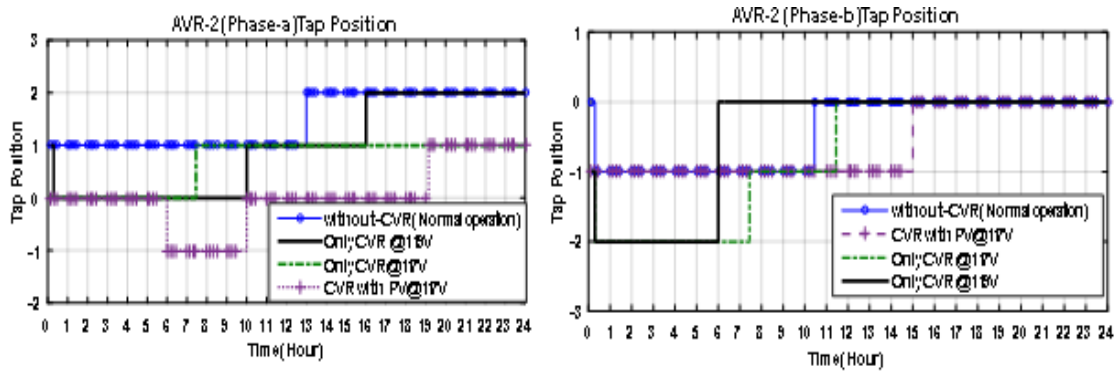


Figure 3.16 Tap Positions of AVR-2 ( in Case II for whole day operation)

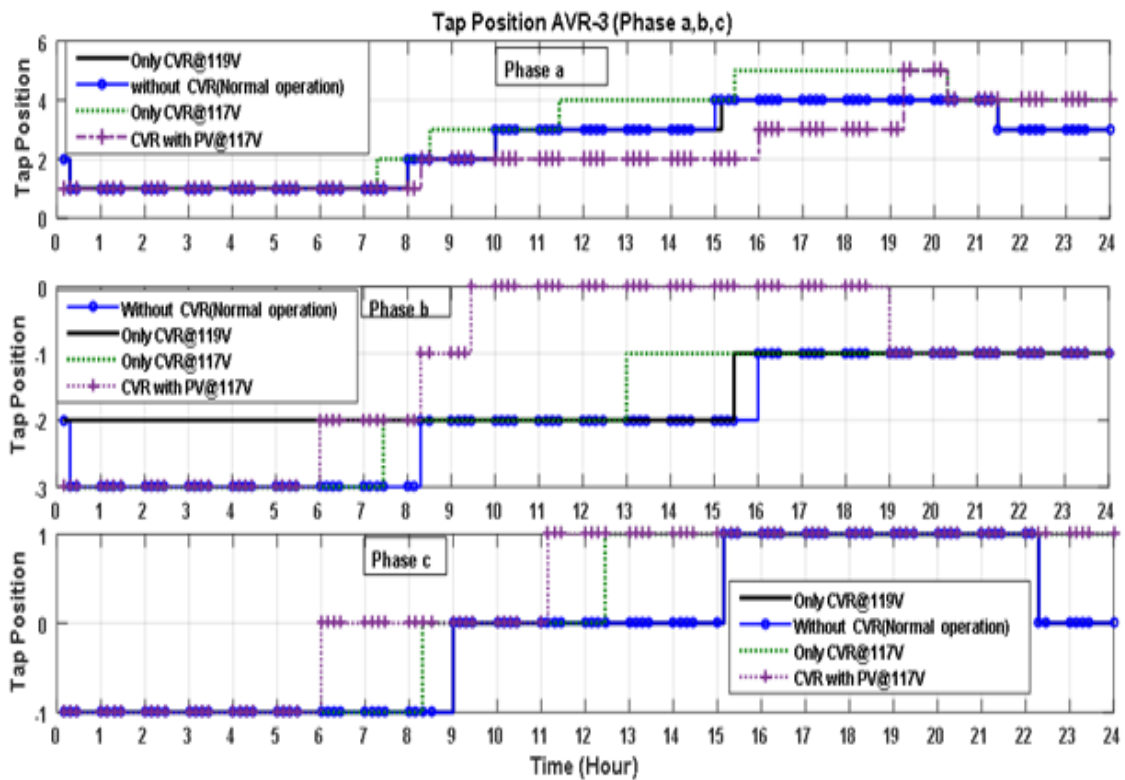


Figure 3.17 Tap Positions of AVR-3 in Case II for whole day operation

### 3.6.3 Moving Cloud Effect

The partial clouds affect the output of the PV system. The effect of partial cloudy day on the power output of PV system under Mode 3 operation has also been studied in both the cases. Figure 3.8 and Figure 3.12 exhibit the active & reactive power supplied by the system in Case 1 and Case 2 respectively. It can clearly be noticed from these figures that power output is fluctuating in nature because of movement of clouds on PV arrays. The

sudden fall in PV power output followed by a rise in power output indicate the interventions of cloud and its disappearance. Consequently, the voltage rise/fall and reversible power flow problem may occur during PV penetrations.

### **3.6 Conclusion**

The effect of smart grid-enabled CVR with the cooperation of solar PV inverter on energy demand has been studied in this chapter. VVC operation has been carried out without and with a smart grid-enabled CVR to estimate the energy savings. Findings of this investigation are as under:

- Significant energy savings and peak loading relief have been achieved with only CVR.
- The higher energy savings have been achieved with CVR and solar PV systems during deeper level voltage reduction within voltage regulatory range.
- The PV inverter injects the droop controlled reactive power within limits during lower voltage limit violation.
- The effect of inverter losses during reactive power support has also been analyzed.
- Moving clouds effect on PV power output has been analyzed.

It can be concluded that the CVR operation with PV system yields a higher reduction in energy consumptions, peak load demand, and system losses in comparison to only-CVR. Overvoltage can be mitigated if the PV system operates in association with CVR. Lower level PV penetrations are the best solution for handling the fluctuation in PV power output; otherwise, PV system need to be equipped with energy storage. Though implementation of CVR through traditional LDC scheme help to reduce the peak power demand but it does not fully utilize the benefits of CVR and PV technology. Therefore, efficient and optimal coordination among the VVC device is required. In the next *chapter 4*, these issues have been taken care of through optimal CVR operation in the presence of DER and distributed energy storage via VVO method.